Negative Refraction and Imaging in a Triangular-Lattice Metallic Photonic-Crystal Slab *

FENG Shuai(冯帅), SUN Mei(孙梅), REN Cheng(任承), REN Kun(任坤), FENG Zhi-Fang(冯志芳), LI Zhi-Yuan(李志远)**, CHENG Bing-Ying(程丙英), ZHANG Dao-Zhong(张道中)

Beijing National Laboratory for Condensed Matter Physics, Institute of Physics, Chinese Academy of Sciences, Beijing 100080

(Received 10 November 2005)

Imaging properties of a two-dimensional photonic crystal (PC) slab consisting of a triangular lattice of metallic cylinders immersed in a dielectric background are investigated by the finite-difference time-domain technique. With the calculated field patterns of a point source placed in the vicinity of the PC slab and the corresponding equifrequency-surface contours, we find that a high-quality image can form in the opposite side of the slab in the lowest TM-polarized photonic band, and this near-field image is formed mainly by the self-collimation effect.

PACS: 78. 20. Ci, 42. 70. Qs

Negative refraction of electromagnetic (EM) waves have attracted a great deal of attention in the last few years.[1−5] Pendry predicted that a negative index material (NIM) slab, which is characterized by simultaneous negative permittivity and permeability, could make a superlens with a resolution far beyond the diffraction limit, which is inherent in the conventional far-field lens.[1] One prominent example towards an NIM is a metamaterial built from arrays of copper split-ring resonators and copper wire strips.[2,3]

It has been shown that negative refraction can also be achieved in photonic crystals (PCs) with a positive index.[6−17] The physical principles that allow negative refraction arise from the dispersion characteristics of wave propagation in a periodic medium, which can be described by analysing the equifrequency-surface (EFS) contours of the band structures.[6] In particular, Luo *et al.*[7,8] showed that all-angle negative refraction (AANR) could be achieved at the lowest band of two-dimensional (2D) square-lattice PCs and at a wavelength four times larger than the lattice constant. As a result of this AANR, a subwavelength image could be formed in the near-field region of the PC slab. Berrier *et al.*[9] showed that negative refraction and light focusing can be achieved in the infrared wavelengths theoretically and experimentally for the two-dimensional PC consisting of a triangular lattice of air holes in a low-index contrast slab. Up to date, most discussions about the imaging properties of a triangular-lattice PC slab are concerned with the frequencies in the second band. In this Letter, we present that negative refraction and superlensing effect can also be achieved in the lowest TM-polarized photonic band for a triangular-lattice metallic PC slab.

We consider a 2D triangular lattice of metallic cylinders immersed in a dielectric background with the lattice constant a. When the frequency of an EM wave is much lower than the collision frequency of the electrons in the metal, a metal can be described by a frequency-independent conductivity. In this study, we only consider the TM polarization, where the electric field E_z is kept to be parallel to the extension axis of the metallic cylinders (assumed to be the z axis). In all the simulations, the radius of the metallic cylinders keeps to be $r = 0.15a$, and $a = 2\,\mathrm{cm}$. A constant $\sigma = 5.8 \times 10^7\,\mathrm{S/m}$ for the copper conductivity is used and the permittivity of the background material is set to be 14.

First, we employ the finite-difference time-domain (FDTD) method with periodic boundary conditions[18,19] to calculate the band structures and the EFS contours of the above PC. Figure 1(a) shows the calculated band structures. The dashed line represents the light line of the environment shifted to the K point. According to Pendry's theory, when AANR occurs, the frequencies must be under the light line of the environment. We can see from Fig. 1(a) that the metallic cylinders lift the first TM-polarized photonic band and cause a stop band gap at the lowest frequencies. The cutoff frequency of this metallic PC is 0.135 (in units of $2\pi c/a$). The dotted line represents the location of frequency 0.18. We can find from the dotted line that the frequency 0.18 is outside the AANR region, although very near to the upper edge of the AANR region. The frequency 0.186 is located far away from the AANR region.

The EFS contours at several frequencies such as 0.15, 0.18, and 0.186 are demonstrated in Fig. 1(b).

* Supported by the National Key Basic Research Special Foundation of China under Grant Nos 2004CB719804 and 2001CB610402, the National Natural Science Foundation of China under Grant No 10404036, the National Center for Nanoscience and Technology of China under Grant No 2003CB7169, and the Supercomputing Center, CNIC, Chinese Academy of Sciences.

** Email: lizy@aphy.iphy.ac.cn

©2006 Chinese Physical Society and IOP Publishing Ltd

The 0.15 contours is very close to a perfect circle, so that the group velocity at any point of the contour is collimated with the wave vector $\boldsymbol{k}$, indicating that the crystal behaves like an effective homogeneous and isotropic medium of usual positive refractive index at this long wavelength. The 0.18 contour is significantly different from a circle. In most part of the 0.18 contour, which is centred around the ΓK direction, the curve is quite flat and has the surface normal pointing to the ΓK direction, while the surface normal is directed towards the K point near the Brillouin-zone (BZ) edge (line MK). As the group velocity for a given Bloch mode characterized by $\boldsymbol{k}$ is parallel to the EFS normal at this $\boldsymbol{k}$, we can see that the group velocities of the excited Bloch wave modes near the BZ edges (shown as V_{g2}) are pointed towards the K point and correspond to an apparent negative refraction direction for the PC slab, which is assumed to have a surface normal parallel to the ΓK direction.

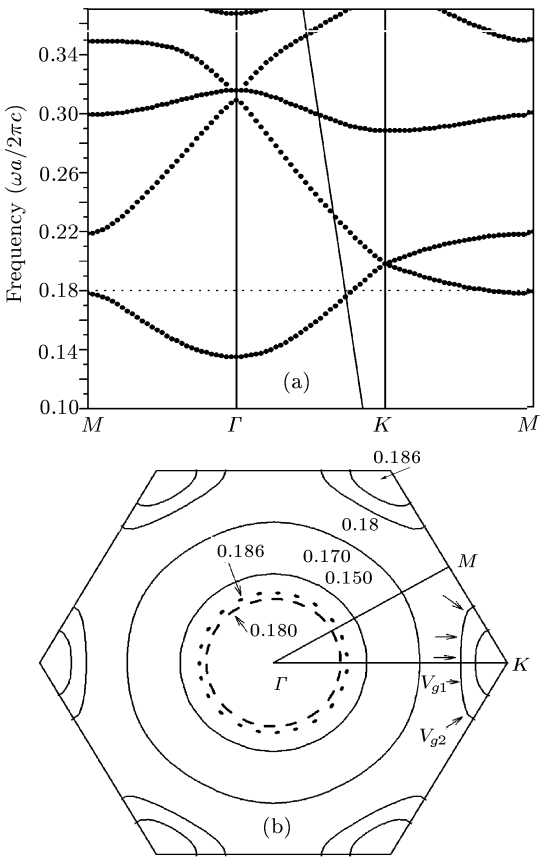


Fig. 1. (a) TM band structures and (b) EFS contours of a 2D PC. The PC is composed of a triangular lattice of metallic cylinders in a dielectric background. The metal has constant conductivity of $\sigma = 5.8 \times 10^7$ S/m. The radius of cylinders is $r = 0.15a$, and $a = 2$ cm. The permittivity of the background material is 14. The dashed line represents the light line of the air environment.

In contrast, the group velocities centred around the ΓK direction (shown as V_{g1}) would point dominantly along the ΓK direction in most part of the contour. The 0.186 contour is similar to the 0.18 contour. The only difference is that the 0.186 curve is slightly distorted from a straight line and is convex with respect to the K point in the most part centred around the ΓK direction, corresponding to a negative refraction direction. The convex degree of the 0.186 curve becomes heavier when the curve moves to the BZ edges. For comparison, we also give the EFS contours at frequencies 0.18 and 0.186 for the air background, which are shown by the dashed and dotted circles in Fig. 1(b), respectively.

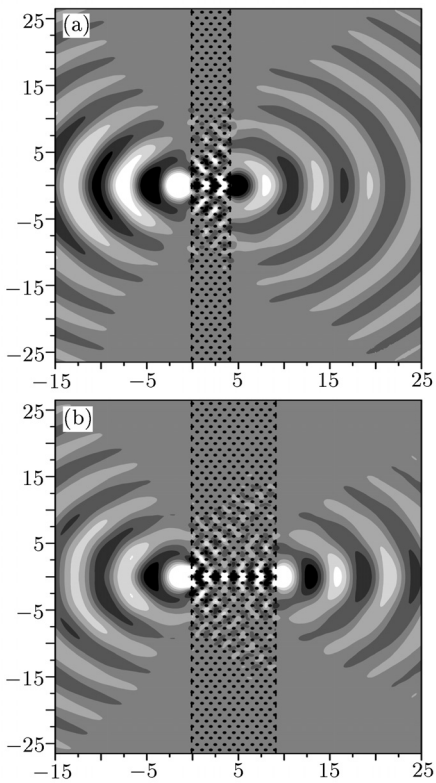


Fig. 2. E_z field patterns of a point source and its image across a metallic PC slab. The rectangular PC slabs are in width of 61 layers and in thicknesses: (a) 9 layers, (b) 19 layers. The slab surface normal is along the K direction. The distance from the left and right slab edges to the centre of the adjacent cylinders is $0.1a$. The point source is placed at $x = -a$ and $y = 0$, and resonant at $\omega = 0.18$ (in units of $2\pi c/a$). The slab surfaces are represented by two dashed lines. Dark and bright regions correspond to negative and positive E_z, respectively.

Secondly, we employ the FDTD method with a boundary treatment of perfectly matched layers to visualize the propagation of EM waves through this kind of metallic PC slab. The rectangular metallic PC slab we consider is in width 61 layers and thickness 9 layers, and the surface normal is along the ΓK direction. The whole PC slab is embedded in the air environment. A point source of continuous wave resonant at $\omega = 0.18$ is placed at the left side of the PC slab and

fixed at $x = -a$ and $y = 0$. The centre of the metallic cylinders in the first layer is located at $x = 0$, and the slab is symmetric with respect to $y = 0$. The distances from the left and right slab edges to the center of the adjacent cylinders are both $0.1a$. The calculated E_z field pattern is displayed in Fig. 2(a). We see that the EM wave radiated from a point source forms a high-quality image in the opposite side of the PC slab. The size of this image (full size at half maximum) is about $2.4a$, corresponding to 0.432λ. We have changed the amount of the cut, while keeping other parameters just the same as described above, and calculated the corresponding field patterns. Visible image spots can also be formed in the right side of the PC slab, but the qualities of these image spots degrade to some extent. The reason is that the PC slab lens with an optimum termination can minimize the reflection between the air-slab interfaces. Thus a high-quality image spot can be achieved.

Then we change the thickness of the above PC slab to be 19 layers, while keeping other parameters unchanged. The background material still cut the outermost layer of cylinders by an amount of $0.05a$. The calculated field pattern is shown in Fig. 2(b), from which we can see that a good-quality image spot also forms in the opposite side of the PC slab. The width of this image is about $2.9a$, corresponding to 0.522λ. No apparent focusing of the EM wave is found inside the slab. Instead, there is a bright channel connecting the point source and the image. This indicates that the self-collimation effect that has been found in dielectric photonic crystals[10] also plays an important role here. Besides the central bright channel, some wave powers from the point source are dispersed across the PC slab along other directions.

The above-mentioned wave propagation behaviour is consistent with the analysis on the EFS contour. The bright channel connecting the image spot and the point source is parallel to the direction of the group velocity V_{g1}. We can attribute this wave beam to coupling of the incident energy power into the Bloch modes in the wide area centred nearly in the ΓK direction of the 0.18 EFS contour. The two weak wave beams propagating within the PC slabs are strongly inclined from the surface normal of the PC slab in a way consistent with the direction of the group velocity V_{g2}. We have attributed these wave beams to coupling of the incident energy power into the Bloch modes located in the small region near the MK direction of the 0.18 EFS contour.

Now we alter the frequency of the point source to be 0.186. The point source is placed at $x = -1.5a$ and $y = 0$, while the other parameters of the PC slab keep unchanged. The calculated E_z field distributions are shown in Figs. 3(a) and 3(b) for the 9- and 19-layer samples. From Fig. 3(a) we can find a good-quality image spot formed in the right side of the PC slab. Compared with the image shown in Fig. 2(a), this image is slightly elongated in the lateral direction, while contracted in the longitudinal direction. The width of this image spot is about $3.3a$, corresponding to 0.614λ. The possible reason for the degradation of the imaging quality is that this frequency is much more above the light line of the environment. The reason for the degradation of the imaging quality again can be visualized from the EFS characteristics of the photonic crystal. As can be found in Fig. 1(b), although the frequency 0.186 is only slightly far away from the light line of the environment than the frequency 0.18, the corresponding 0.186 EFS contour within the photonic crystal is much more contracted towards the BZ edge, and runs across a BZ area much smaller than the 0.18 EFS contour. By comparing the EFSs of the frequency 0.18 in air and in PC, we find that almost all the EM waves radiated from the point source can transmit the PC slab either through a collimation direction (for wave components with small incident angles) or through a negative refraction direction (for wave components with large incident angles). In contrast, when the frequency becomes 0.186, quite a part of the EM

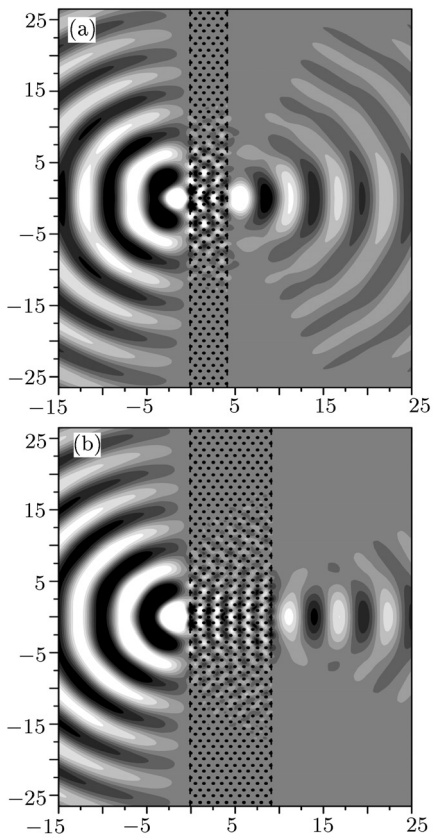


Fig. 3. The same as Fig. 2 but the frequency of the point source becomes 0.186, and the source is located at $x = -1.5a$ and $y = 0$.

waves radiated from the point source (with large incident angles) cannot excite Bloch modes within the PC structure, so they cannot transmit through the PC slab and will finally be reflected. As a high-quality image spot requires as much as possible wave components transmitting the PC slab, increasing the frequency of the point source from 0.18 to 0.186 will lead to the imaging degradation.

When the thickness of the PC slab becomes 19 layers, we can see from Fig. 3(b) that a visible image spot is also formed on the right side of PC slab, but with a still degraded quality. The width of this image spot is about $5.0a$, corresponding to 0.93λ. The bright channel inside the PC slab becomes narrower when it transverses across the PC slab. This is also consistent with the analysis of the EFS contour of the frequency 0.186. The good consistence between the FDTD simulation of the wave propagation behaviour and the EFS contour analysis on Bloch wave modes once again demonstrates that the EFS is a very useful physical quantity to understand the main properties of EM wave propagation in PC structures.

In summary, we have investigated the imaging properties of EM waves by 2D PC slabs consisting of a triangular lattice of metallic cylinders immersed in a dielectric background. From the analysis of the EFS contours and the field patterns of a point source placed in the vicinity of the PC slab, we find that a high-quality image is formed in the opposite side of the PC slab. This image is formed not only by the negative refractive effect, but also mainly by the self-collimation effect. In addition, high-quality images can form at frequencies in the fundamental band and above the light line of the environment, in a way beyond the expectation from the AANR mechanism.

References

[1] Pendry J B 2000 *Phys. Rev. Lett.* **85** 3966
[2] Shelby R A, Smith D R and Schultz S 2001 *Science* **292** 77
[3] Houck A A, Brock J B and Chuang I L 2003 *Phys. Rev. Lett.* **90** 137401
[4] Smith D R and Schurig D 2003 *Phys. Rev. Lett.* **90** 077405
[5] Li J, Zhou L, Chan C T and Sheng P 2003 *Phys. Rev. Lett.* **90** 083901
[6] Zhang X D and Li L M 2005 *Appl. Phys. Lett.* **86** 121103
[7] Luo C, Johnson S G, Joannopoulos J D and Pendry J B 2002 *Phys. Rev.* B **65** 201104(R)
[8] Luo C, Johnson S G, Joannopoulos J D and Pendry J B 2003 *Phys. Rev.* B **68** 045115
[9] Berrier A, Mulot M, Swillo M, Qiu M, Thylen L, Talneau A and Anand S 2004 *Phys. Rev. Lett.* **93** 073902
[10] Li Z Y and Lin L L 2003 *Phys. Rev.* B **68** 245110
[11] Zhang X D 2004 *Phys. Rev.* B **70** 205102
[12] Wheeler M S, Aitchison J S and Mojahedi M 2005 *Phys. Rev.* B **71** 155106
[13] He S, Ruan Z C, Chen L and Shen J Q 2004 *Phys. Rev.* B **70** 115113
[14] Feng Z F, Zhang X D, Wang Y Q, Li Z Y, Cheng B Y and Zhang D Z 2005 *Phys. Rev. Lett.* **94** 247402
[15] Feng S, Li Z Y, Feng Z F, Cheng B Y and Zhang D Z 2005 *Phys. Rev.* B **72** 075101
[16] Feng S, Li Z Y, Feng Z F, Ren K, Cheng B Y and Zhang D Z 2005 *J. Appl. Phys.* **98** 063102
[17] Fang Y T and Shen T G 2005 *Chin. Phys. Lett* **22** 949
[18] Yee K S 1966 *IEEE Trans. Antenna Propag.* **14** 302
[19] Berenger J P 1994 *J. Comput. Phys.* **114** 185